Overall Kinetic Mechanism of Saccharopine Dehydrogenase from *Saccharomyces cerevisiae*†

Hengyu Xu, Ann H. West, and Paul F. Cook*

Department of Chemistry and Biochemistry, University of Oklahoma, 620 Parrington Oval, Norman, Oklahoma 73019

Received May 31, 2006; Revised Manuscript Received July 13, 2006

ABSTRACT: Kinetic data have been measured for the histidine-tagged saccharopine dehydrogenase from *Saccharomyces cerevisiae*, suggesting the ordered addition of nicotinamide adenine dinucleotide (NAD) followed by saccharopine in the physiologic reaction direction. In the opposite direction, the reduced nicotinamide adenine dinucleotide (NADH) adds to the enzyme first, while there is no preference for the order of binding of α-ketoglutarate (α-Kg) and lysine. In the direction of saccharopine formation, data also suggest that, at high concentrations, lysine inhibits the reaction by binding to free enzyme. In addition, uncompetitive substrate inhibition by α-Kg and double inhibition by NAD and α-Kg suggest the existence of an abortive E:NAD:α-Kg complex. Product inhibition by saccharopine is uncompetitive versus NADH, suggesting a practical irreversibility of the reaction at pH 7.0 in agreement with the overall K_{eq}. Saccharopine is noncompetitive versus lysine or α-Kg, suggesting the existence of both E:NADH:saccharopine and E:NAD:saccharopine complexes. NAD is competitive versus NADH, and noncompetitive versus lysine and α-Kg, indicating the combination of the dinucleotides with free enzyme. Dead-end inhibition studies are also consistent with the random addition of α-Kg and lysine. Leucine and oxalylglycine serve as lysine and α-Kg dead-end analogues, respectively, and are uncompetitive against NADH and noncompetitive against α-Kg and lysine, respectively. Oxaloacetate (OAA), pyruvate, and glutarate behave as dead-end analogues of lysine, which suggests that the lysine-binding site has a higher affinity for keto acid analogues than does the α-Kg site or that dicarboxylic acids have more than one binding mode on the enzyme. In addition, OAA and glutarate also bind to free enzyme as does lysine at high concentrations. Glutarate gives S-parabolic noncompetitive inhibition versus NADH, indicating the formation of a E:$(\text{glutarate})_2$ complex as a result of occupying both the lysine- and α-Kg-binding sites. Pyruvate, a slow alternative keto acid substrate, exhibits competitive inhibition versus both lysine and α-Kg, suggesting the combination to the E:NADH:α-Kg and E:NADH:lysine enzyme forms. The equilibrium constant for the reaction has been measured at pH 7.0 as 3.9×10^{-7} M by monitoring the change in NADH upon the addition of the enzyme. The Haldane relationship is in very good agreement with the directly measured value.

Saccharopine dehydrogenase [SDH;[1] *N*6-(glutaryl-2)-L-lysine:nicotinamide adenine dinucleotide (NAD) oxidoreductase (L-lysine forming); (EC 1.5.1.7)] catalyzes the final step in the α-aminoadipate pathway (AAA) for lysine biosynthesis (*1*, *2*). The AAA pathway, a member of the glutamate family of amino acid biosynthesis (*3*), is unique in euglenoids and higher fungi, with α-ketoglutarate (α-Kg) serving as the precursor for L-lysine (*4*−*7*). Human pathogens such as *Candida albicans*, *Cryptococcus neoformas*, and *Aspergillus fumigatus* and plant pathogens such as *Magnaporthe grisea* use the pathway to synthesize lysine (*8*, *9*). The uniqueness of the AAA pathway makes it a target for the rapid detection and control of pathogenic yeasts and molds. Selective inhibition of the enzyme(s) of this pathway by an appropriate inhibitor may control or eradicate the growth of fungal pathogens *in vivo* (*8*, *10*).

SDH catalyzes the reversible pyridine nucleotide-dependent oxidative deamination of saccharopine to generate α-Kg and lysine using NAD as an oxidizing agent (eq 1; see ref *1*). The enzyme from *Saccharomyces cerevisiae* is a monomer with a reported molecular weight of ∼39 000 and contains one binding site for reactants (*11*).

The *S. cerevisiae* enzyme has pH optima of 10.0 in the direction of lysine formation and 7.0 in the direction of saccharopine formation (*2*, *12*). The K_m values for NAD, saccharopine, lysine, α-Kg, and reduced nicotinamide adenine dinucleotide (NADH) have been estimated as 0.1, 1.7, 2, 0.55, and 0.089 mM, respectively (*2*). Previous studies of the kinetic mechanism of the SDH suggested an ordered Bi-Ter kinetic mechanism with NAD binding first, followed by saccharopine, and products released in the order of lysine, α-Kg, and NADH (*1*, *2*, *13*, *14*). However, one of the three initial velocity patterns obtained by the authors (*12*), the one

† This work is supported by a grant from the National Institute of Health GM 071417 to P.F.C. and A.H.W. and the Grayce B. Kerr Endowment to the University of Oklahoma (to P.F.C.).

* To whom correspondence should be addressed. E-mail: pcook@chemdept.chem.ou.edu. Telephone: 405-325-4581. Fax: 405-325-7182.

[1] Abbreviations: SDH, saccharopine dehydrogenase; AAA, α-aminoadipate pathway; α-Kg, α-ketoglutarate; OG, oxalylglycine; OAA, oxaloacetate; NAD, nicotinamide adenine dinucleotide (the + charge is omitted for convenience); NADH, reduced nicotinamide adenine dinucleotide; Hepes, 4-(2-hydroxyethyl)-1-piperazine-ethanesulfonic acid; C, competitive; UC, uncompetitive; NC, noncompetitive; ITC, isothermal titration calorimetry; LB, Luria−Bertani; Amp, ampicillin; IPTG, isopropyl-β-D-1-thiogalactopyranoside.

10.1021/bi0610808 CCC: $33.50
Published on Web 09/12/2006

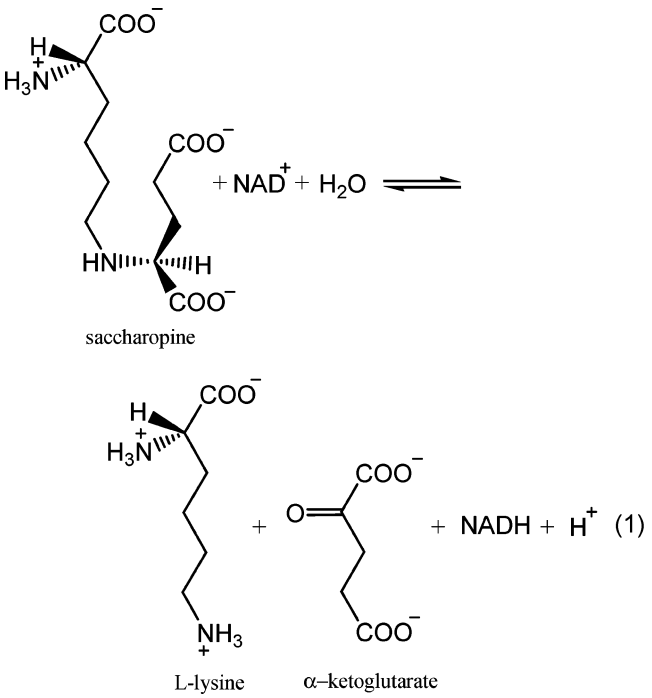

with NADH and lysine varied at saturating α-Kg, was not consistent with the proposed ordered mechanism. In addition, these investigators demonstrated that the SDH is capable of catalyzing the reaction using pyruvate in place of α-Kg as a substrate but with products released in the order pyruvate, lysine, and NADH, opposite that obtained with saccharopine as a substrate (*15*, *16*). Reversal in the order of release of lysine and the keto acid substrate suggests randomness in substrate binding. Considering that all substrates must add to the enzyme prior to reaction, SDH was proposed to have separate binding subsites for the coenzyme, keto, and amino acid substrates in the direction of reductive amination (*1*).

Kinetic analysis of the SDH reaction in the presence of reactants and inhibitors provides information on the kinetic mechanism and features of the substrate-binding sites. A number of questions were raised after a consideration of previous data, and the proposed mechanism was considered suspect. In this paper, we report initial rate studies that define the overall kinetic mechanism of the SDH from *S. cerevisiae*. Data are discussed in terms of potential rate-limiting steps along the reaction pathway and are used to estimate the equilibrium constant using the Haldane relationship, which is compared to the value obtained directly.

MATERIALS AND METHODS

Chemicals. All chemicals were of the highest grade commercially available and were used without further purification. L-Saccharopine, L-lysine, L-leucine, α-Kg, glutarate, oxaloacetate (OAA), pyruvate, imidazole, and chloramphenicol were obtained from Sigma. β-NADH, β-NAD, Luria−Bertani (LB) broth, and LB agar were purchased from USB. The Ni−NTA agarose resin was from Qiagen. Isopropyl-β-D-1-thiogalactopyranoside (IPTG), *Sma*I, *Nde*I, *Bam*HI, Platinum Pfx polymerase, and T4 DNA ligase were from Invitrogen. Ampicillin (Amp) was from Fisher Biotechnologies, and 4-(2-hydroxyethyl)-1-piperazine-ethanesulfonic acid (Hepes) was from Research Organics. Oxalylglycine (OG) was from Frontier Scientific.

Molecular Cloning, Cell Growth, and Protein Expression. A 1154 bp DNA fragment encoding SDH was amplified by polymerase chain reaction (PCR) with 200 ng of yeast genomic DNA as the template using the following protocol: one cycle of initial denaturation at 94 °C for 2 min, followed by 35 cycles of denaturation at 94 °C for 45 s, annealing at 50 °C for 45 s, and extension at 72 °C for 3 min. The enzyme used was Platinum Pfx polymerase, which produces blunt-end PCR products. The pUC12 cloning vector was digested with *Sma*I to create a blunt-end linear vector that was gel-purified. The purified *Lys1* DNA was ligated into linearized pUC12 vector. *Escherichia coli* DH5α cells were transformed with the plasmid, and single colonies were grown on LB/Amp medium. Plasmids from each clone were isolated, and restriction endonuclease mapping was carried out on the plasmids to confirm the presence of the insert.

For subcloning into the expression vector, the *Lys1* insert was excised from the pUC12-*Lys1* plasmid with *Nde*I/*Bam*HI restriction endonucleases and the digested plasmid was electrophoresed on a 1% agarose gel. The fragment containing the *Lys1* gene was gel-purified and subcloned using T4 ligase into the pET16b expression vector, which was previously digested with *Nde*I/*Bam*HI. *E. coli* BL21 (DE3) RIL cells were then transformed, and the new plasmid was designated sdhHX1. The entire gene was then sequenced at the Laboratory for Genomics and Bioinformatics of the University of Oklahoma Health Science Center in Oklahoma City, OK.

The sdhHX1 plasmid-containing strain was grown at 37 °C in LB supplemented with 100 μg/mL Amp and 25 μg/mL chloramphenicol. Induction by 1 mM IPTG (final concentration) was accomplished once the OD_{600} reached 0.7−0.9. Cell growth was then continued at 32 °C overnight. After centrifugation, the harvested cells were suspended in 100 mM Hepes at pH 7.0 and sonicated on ice for 1.5 min, with a 15 s pulse followed by a 30 s rest, using a MISONIX Sonicator XL. After the cell debris was removed by centrifugation at 12000*g* for 15 min, the collected supernatant was mixed with the Ni−NTA resin at 4 °C, washed with 20 mM imidazole at pH 7.0, and then eluted with buffer containing 300 mM imidazole at pH 7.0. The SDH-containing sample, identified by SDS−PAGE, was concentrated using an Amicon ultrafiltration device with a YM 10 membrane.

Enzyme Assay. The SDH reaction was followed by measuring the appearance or disappearance of NADH at 340 nm (ϵ_{340} = 6220 M^{-1} cm^{-1}) using a Beckman DU 640 spectrophotometer. All assays were carried out at 25 °C, and the temperature was maintained by a Neslab RTE-111 circulating water bath. A unit of enzyme activity is defined as the amount of enzyme catalyzing the production or utilization of 1 μmol of NADH/min at 25 °C. The rate measurements were all carried out in 1.0 mL of 100 mM Hepes at pH 7.0. The reactions were initiated by addition of 10 μL of an appropriately diluted enzyme solution (∼1.4 μM final concentration) to a mixture that contained all other reaction components in a 1 mL volume, and the initial linear portion of the time course was used to calculate the initial velocity. Because the diluted enzyme solution (protein concentrations less than 100 μg/mL) is not stable, 50% glycerol was added to the enzyme solution to minimize any

activity loss, and the diluted enzyme solution was prepared fresh daily.

Initial Velocity Studies: Systematic Analysis. The initial rate in the direction of saccharopine formation was measured as a function of the NADH concentration (0.015−0.2 mM), different fixed concentrations of α-Kg (0.1−1 mM), and a fixed concentration of L-lysine (0.5 mM). The experiment was then repeated at several additional L-lysine concentrations (0.71−5 mM). Initial velocity studies were also carried out in the direction of saccharopine oxidation at pH 7.0. In this case, the initial rate was measured as a function of NAD (0.2−2 mM) at different fixed levels of saccharopine (5−50 mM). The amount of enzyme used for each reaction in the direction of saccharopine oxidation was twice that used in the reverse reaction.

Pairwise Analysis. Initial rates were measured varying one substrate at different fixed concentrations of a second and with the third substrate saturating. For example, the initial rate was measured as a function of NADH at several fixed levels of α-Kg and with lysine fixed at $10K_m$. The fixed saturating concentrations of NADH, α-Kg, and L-lysine were 0.2 mM ($5K_m$), 5 mM ($20K_m$), and 12.5 mM ($10K_m$), respectively.

Substrate Inhibition. Lysine substrate inhibition studies were carried out by measuring the initial rates as a function of the lysine concentration (5−200 mM), with the concentration of the other two substrates both fixed at their respective K_m values. In the case of α-Kg substrate inhibition, the initial rates were measured as a function of the NADH concentration and different fixed α-Kg concentrations (0.1−50 mM) and with the lysine concentration fixed at 6 times its K_m value.

Product and Dead-End Inhibition Studies. Inhibition patterns were obtained by measuring the initial rate at different concentrations of one reactant, with the concentration of the other reactants fixed at different levels (see Table 2), and at different fixed concentrations of the inhibitor including 0. In all cases, an initial estimate of the K_i for the inhibitor was obtained by fixing the varied substrate at its K_m value and varying the inhibitor concentration. The appK_i is estimated by Dixon analysis, a plot of $1/v$ versus **I**, extrapolating to $1/v$ equal to 0, and dividing by 2.

Double Inhibition. A double-inhibition study was performed to investigate the existence of the E:NAD:α-Kg dead-end complex. The initial rates were measured as a function of NAD (0−8 mM) at different fixed levels of α-Kg (20−50 mM), with the concentration of the other substrates, NADH and lysine, both fixed at their respective K_m values.

Data Analysis. Initial velocity data were first analyzed graphically using double-reciprocal plots of initial velocities versus substrate concentrations and suitable secondary and tertiary plots. Data were then fitted using the appropriate equation and the Marquardt−Levenberg algorithm (*17*), supplied with the EnzFitter program from BIOSOFT, Cambridge, U.K. Kinetic parameters and their corresponding standard errors were estimated using a simple weighting method.

Data obtained from the systematic analysis in the direction of saccharopine formation were fitted using eqs 2 and 3 for a terreactant kinetic mechanism (*18*). In the direction of saccharopine oxidation, data were fitted using eq 4. The three data sets obtained from the pairwise analysis in the direction of saccharopine formation were fitted using either eq 4 for a sequential mechanism or eq 5 with the constant term absent. Data conforming to competitive (C) , noncompetitive (NC), or uncompetitive (UC) inhibition were fitted using eqs 6−8. Data for double inhibition by NAD and α-Kg were fitted using eq 9. Data for glutarate inhibition against NADH were fitted using eq 10.

$$v = [V\mathbf{ABC}]/ [\text{constant} + (\text{coefA})\mathbf{A} + (\text{coefB})\mathbf{B} + (\text{coefC})\mathbf{C} + K_c\mathbf{AB} + K_b\mathbf{AC} + K_a\mathbf{BC} + \mathbf{ABC}] \quad (2)$$

$$v = \frac{V\mathbf{ABC}}{\text{constant} + (\text{coefA})\mathbf{A} + K_c\mathbf{AB} + K_b\mathbf{AC} + K_a\mathbf{BC} + \mathbf{ABC}} \quad (3)$$

$$v = \frac{V\mathbf{AB}}{K_{ia}K_b + K_a\mathbf{B} + K_b\mathbf{A} + \mathbf{AB}} \quad (4)$$

$$v = \frac{V\mathbf{AB}}{K_a\mathbf{B} + K_b\mathbf{A} + \mathbf{AB}} \quad (5)$$

$$v = \frac{V\mathbf{A}}{K_a\left(1 + \frac{\mathbf{I}}{K_{is}}\right) + \mathbf{A}} \quad (6)$$

$$v = \frac{V\mathbf{A}}{K_a\left(1 + \frac{\mathbf{I}}{K_{is}}\right) + \mathbf{A}\left(1 + \frac{\mathbf{I}}{K_{ii}}\right)} \quad (7)$$

$$v = \frac{V\mathbf{A}}{K_a + \mathbf{A}\left(1 + \frac{\mathbf{I}}{K_{ii}}\right)} \quad (8)$$

$$v = \frac{v_0}{1 + \frac{\mathbf{I}}{K_i} + \frac{\mathbf{J}}{K_j} + \frac{\mathbf{IJ}}{\alpha K_i K_j}} \quad (9)$$

$$v = \frac{\mathrm{V}\mathbf{A}}{K_a\left(1 + \frac{\mathbf{I}^2}{K_{is}^2}\right) + \mathbf{A}\left(1 + \frac{\mathbf{I}}{K_{ii}}\right)} \quad (10)$$

In eqs 2−10, v and V are initial and maximum velocities, **A**, **B**, and **C** are substrate concentrations, **I** and **J** are inhibitor concentrations, and K_a, K_b, and K_c are Michaelis constants for substrates A, B, and C, respectively. In eqs 1 and 2, the constant and coef terms are products of kinetic constants that depend on the kinetic mechanism and will be defined in the Discussion. In eq 4, K_{ia} is the dissociation constant of A from the EA complex. In eqs 6−8, K_{is} and K_{ii} represent inhibition constants for the slope and intercept, respectively. In eq 9, K_i and K_j are dissociation constants for EI and EJ complexes, respectively, and v_0 is the rate in the absence of inhibitors and α is the interaction constant that estimates the influence of one inhibitor upon binding of the other. In eq 10, K_{is} is the average dissociation constant for glutarate from the E:glutarate and E:(glutarate)$_2$ complexes, and all other terms are the same as defined above.

Determination of K_{eq} and the Haldane Relationship. In a 1 mL reaction mixture, the concentrations of NADH, α-Kg,

Table 1: Kinetic Parameters of SDH at pH 7.0

forward reaction	
K_{NAD} (mM)	0.9 ± 0.1
K_{sacc} (mM)	6.7 ± 1.4
K_{iNAD} (mM)	1.1 ± 0.3
V_1/E_t (s^{-1})	1.1 ± 0.1
$V_1/K_{NAD}E_t$ (M^{-1} s^{-1})	$(1.2 \pm 0.1) \times 10^3$
$V_1/K_{sacc}E_t$ (M^{-1} s^{-1})	$(1.6 \pm 0.3) \times 10^2$
reverse reaction	
K_{NADH} (mM)	0.019 ± 0.002
K_{Lys} (mM)	1.1 ± 0.2
$K_{\alpha-Kg}$ (mM)	0.11 ± 0.03
constant $(mM)^3$	0.013 ± 0.002
coefA $(mM)^2$	0.71 ± 0.08
V_2/E_t (s^{-1})	20 ± 1
$V_2/K_{NADH}E_t$ (M^{-1} s^{-1})	$(1.6 \pm 0.2) \times 10^6$
$V_2/K_{Lys}E_t$ (M^{-1} s^{-1})	$(2.5 \pm 0.4) \times 10^4$
$V_2/K_{\alpha-Kg}E_t$ (M^{-1} s^{-1})	$(2.8 \pm 0.7) \times 10^5$
substrate inhibition	

varied substrate	substrate inhibitor	K_I (mM)	inhibition pattern
NADH	L-lysine	27.8 ± 0.3	C
NADH	α-Kg	28 ± 7	UC

L-lysine, and saccharopine were fixed at 0.05, 0.1, 0.1, and 2.5 mM, respectively, and the concentration of NAD was varied over the range of 0.1−5 mM in separate reactions. The reaction was initiated by the addition of enzyme. The difference in A_{340} representing the displacement from equilibrium was plotted against the NAD concentration. The K_{eq} is obtained using the concentrations given above and the concentration of NAD that gave a ΔA_{340} of 0 according to eq 11

$$K_{eq} = \frac{[NADH][\alpha\text{-Kg}][\text{L-lysine}]}{[NAD][\text{saccharopine}]} \quad (11)$$

The K_{eq} was also estimated from the Haldane relationship for a Bi-Ter kinetic mechanism according eq 12

$$K_{eq} = \frac{\frac{V}{K_{sacc}}K_{iNADH}K_{iLys}}{\frac{V}{K_{\alpha-Kg}}K_{iNAD}} \quad (12)$$

where K_{iNADH}, K_{iNAD}, and K_{iLys} are inhibition constants for the respective reactants and all other terms are as defined above.

RESULTS

Cell Growth, Protein Expression, and Purification. The expression of SDH is very high under conditions used to induce expression. After the enzyme is washed with 20 mM imidazole, it is eluted from the Ni−NTA column most efficiently by 300 mM imidazole, and the purity of the eluted SDH is about 98% by densitometric scanning (data not shown). The amount of purified enzyme obtained is 35−40 mg from a 200 mL cell culture (500 mg wet cell pellet). His-tagged SDH is active and stable for months when kept at 4 °C at concentrations ≥0.1 mg/mL and pH 7.0.

Initial Velocity Studies: Systematic Analysis. Double-reciprocal initial velocity patterns in the direction of saccharopine formation were obtained by varying the concentration of NADH and α-Kg at different fixed concentrations

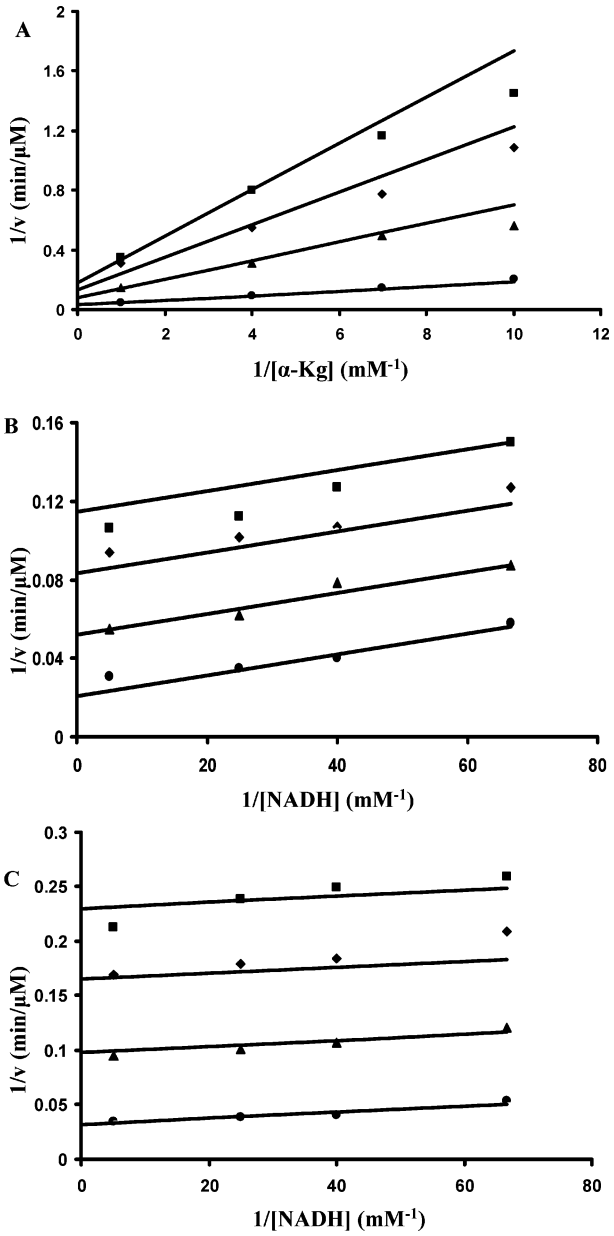

FIGURE 1: Pairwise analysis of the SDH oxidative deamination reaction. Double-reciprocal plots obtained upon varying one substrate at different fixed concentrations of a second and with the third substrate saturating. Rates were measured in 100 mM Hepes at pH 7.0 and 25 °C. (A) Initial velocity pattern obtained with the α-Kg/lysine pair with NADH at 0.2 mM ($5K_{NADH}$). (B) Initial velocity pattern obtained for the NADH/α-Kg pair with lysine at 12.5 mM ($10K_{Lys}$). (C) Initial velocity pattern obtained for the NADH/lysine pair with α-Kg at 5 mM ($20K_{\alpha-Kg}$). The points are experimental, while the solid lines are theoretical based on a fit to eq 4 in A and to eq 5 in B and C.

of lysine. The crossover points for all double-reciprocal plots are to the left of the ordinate (data not shown). All of the initial velocity data were fitted to the equation for a fully random terreactant mechanism (eq 2) to determine which terms, if any, in the denominator of the rate equation were absent. Data were then fitted to eq 3, which describes a kinetic mechanism with ordered addition of A followed by random addition of B and C. Values of the kinetic parameters determined were identical to those obtained using eq 2, and the standard error of the fit was also identical.

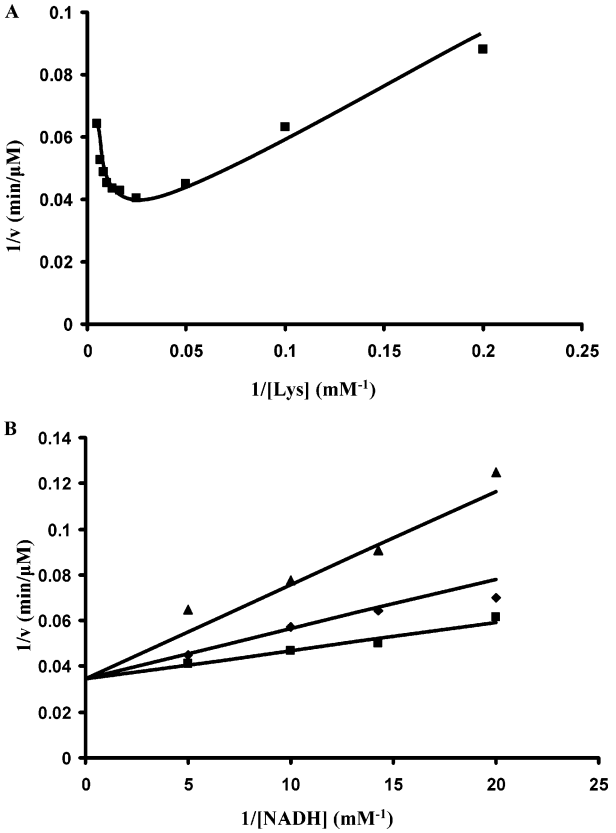

FIGURE 2: Competitive substrate inhibition by lysine against NADH. (A) Plot of the reciprocal initial rate versus the lysine concentration, with the other substrates fixed at their respective K_m. (B) Double-reciprocal plot exhibiting competitive substrate inhibition by lysine [100 mM (■), 200 mM (◆), and 400 mM (▲)] versus NADH, with α-Kg fixed at its K_m. Rates were measured in 100 mM Hepes at pH 7.0 and 25 °C. The points are experimental, while the solid lines are theoretical based on a fit to eq 4 in A and to eq 6 in B.

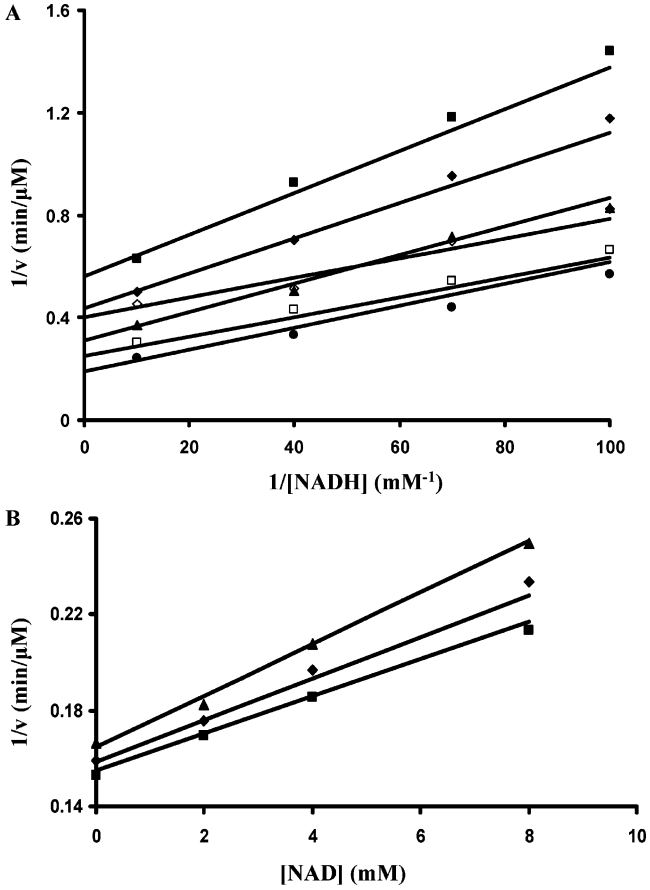

FIGURE 3: Substrate inhibition by α-Kg against NADH. (A) Uncompetitive inhibition by α-Kg versus NADH. The concentrations of α-Kg were 0.1 mM (■), 0.143 mM (◆), 0.25 mM (▲), 1 mM (●), 20 mM (□), and 50 mM (◇). The concentration of lysine is fixed at 5 mM. (B) Double inhibition by NAD and α-Kg. Plot of the reciprocal initial rate versus the NAD concentration (0−8 mM) at different levels of α-Kg [20 mM (■), 30 mM (◆), and 50 mM (▲)]. The points are experimental, while the solid lines are theoretical based on a fit to eq 8 in A and to eq 9 in B.

Initial rates were also obtained in the direction of saccharopine oxidation at pH 7.0, as a function of the NAD concentration and different fixed levels of saccharopine. The pattern intersects to the left of the ordinate (data not shown). Estimates of all of the kinetic parameters in this reaction direction were obtained by fitting the data to eq 4 for a sequential mechanism. All kinetic parameters for both reaction directions are summarized in Table 1. Values of K_{NADH}, K_{Lys}, and $K_{\alpha-Kg}$ are identical, within error, to those reported previously (*2*).

Pairwise Analysis. To further define the kinetic mechanism, initial velocity patterns obtained by varying one substrate at different fixed concentrations of a second and with the third substrate saturating were obtained and are shown in parts A−C of Figure 1. An intersecting initial velocity pattern was observed for the α-Kg/lysine pair (Figure 1A), while the NADH/α-Kg and NADH/lysine pairs gave parallel patterns (parts B and C of Figure 1). Patterns are consistent with the ordered addition of NADH followed by the random addition of α-Kg and lysine. Kinetic parameters were obtained by fitting the data to eqs 4 and 5. Values of kinetic parameters were in good agreement with those obtained via the systematic analysis described above.

Substrate Inhibition. When the initial rate was measured over a wide range of lysine concentrations (5−200 mM), with the concentrations of the other two substrates fixed at their respective K_m, the double-reciprocal plot exhibits substrate inhibition as the lysine concentration increases above 60 mM (Figure 2A). Inhibition by lysine versus NADH is competitive (Figure 2B). Substrate inhibition constants are summarized in Table 1.

The initial velocity pattern obtained with lysine at 6 times its K_m and NADH varied at different fixed concentrations of α-Kg exhibits substrate inhibition that is uncompetitive versus NADH (Figure 3A). Data suggest the binding of α-Kg to the E:NAD complex. A double-inhibition experiment obtained with NADH and lysine fixed at their K_m values and NAD and α-Kg varied is consistent with the formation of an E:NAD:α-Kg complex (Figure 3B). The rate in the absence of inhibitors, v_0, was 6.7 ± 0.2 μM/min. The dissociation constants for E:NAD and E:α-Kg complexes are 26 ± 5 and 460 ± 160 mM, respectively. The interaction constant α was 0.12 ± 0.09, indicating synergism of binding for NAD and α-Kg.

Product Inhibition Studies. Product inhibition data in both reaction directions are summarized in Table 2. In the direction of saccharopine formation, saccharopine is uncompetitive versus NADH and noncompetitive versus lysine and α-Kg, while NAD is competitive versus NADH and noncompetitive versus lysine and α-Kg. In the opposite direction,

Table 2: Inhibition Kinetic Constants for Product Inhibitors of SDH

varied substrate	fixed substrate	inhibitor	K_{is} (mM)	K_{ii} (mM)	inhibition pattern
NADH	L-lysine (K_m) α-Kg ($2K_m$)	saccharopine		1.00 ± 0.05	UC
L-lysine	NADH (K_m) α-Kg ($2K_m$)	saccharopine	1.5 ± 0.1	1.42 ± 0.08	NC
α-Kg	NADH (K_m) L-lysine (K_m)	saccharopine	0.95 ± 0.05	11 ± 4	NC
NADH	L-lysine ($2K_m$) α-Kg ($2K_m$)	NAD	1.56 ± 0.03		C
L-lysine	NADH ($3K_m$) α-Kg ($2K_m$)	NAD	44 ± 4	4.0 ± 0.1	NC
α-Kg	NADH ($3K_m$) L-lysine ($2K_m$)	NAD	28 ± 8	107 ± 96	NC
NAD	saccharopine ($1.5K_m$)	NADH	0.0032 ± 0.0004		C
saccharopine	NAD (K_m)	NADH	0.033 ± 0.003	0.0105 ± 0.0003	NC
NAD	saccharopine ($1.5K_m$)	L-lysine	19 ± 3	33 ± 4	NC
saccharopine	NAD (K_m)	L-lysine	2.84 ± 0.06		C
saccharopine	NAD ($20K_m$)	α-Kg	6.0 ± 0.7	64 ± 6	NC

Table 3: Inhibition Kinetic Constants for Dead-End Inhibitors of SDH

varied substrate	fixed substrate	inhibitor	K_{is} (mM)[a]	K_{ii} (mM)[a]	inhibition pattern
NADH	L-lysine ($2K_m$) α-Kg ($2K_m$)	L-leucine		0.45 ± 0.01 (0.240 ± 0.005)	UC
L-lysine	NADH ($3K_m$) α-Kg ($2K_m$)	L-leucine	0.44 ± 0.03 (0.17 ± 0.01)		C
α-Kg	NADH ($3K_m$) L-lysine ($2K_m$)	L-leucine	1.12 ± 0.26 (0.64 ± 0.15)	0.23 ± 0.02 (0.10 ± 0.01)	NC
NADH	L-lysine ($2K_m$) α-Kg ($2K_m$)	OG		0.06 ± 0.02 (0.020 ± 0.007)	UC
L-lysine	NADH ($3K_m$) α-Kg ($2K_m$)	OG	0.154 ± 0.004 (0.070 ± 0.002)	0.36 ± 0.01 (0.060 ± 0.002)	NC
α-Kg	NADH ($3K_m$) L-lysine ($2K_m$)	OG	0.100 ± 0.002 (0.070 ± 0.001)		C
NADH	L-lysine ($2K_m$) α-Kg ($2K_m$)	OAA	4.7 ± 1.8	11.8 ± 2.6	NC
L-lysine	NADH ($3K_m$) α-Kg ($2K_m$)	OAA	6.1 ± 0.5		C
α-Kg	NADH ($3K_m$) L-lysine ($2K_m$)	OAA	6.4 ± 0.5	29 ± 8	NC
NADH	L-lysine ($2K_m$) α-Kg ($2K_m$)	pyruvate		11.21 ± 0.04	UC
L-lysine	NADH ($3K_m$) α-Kg ($2K_m$)	pyruvate	17.9 ± 0.5		C
α-Kg	NADH ($3K_m$) L-lysine ($2K_m$)	pyruvate	19 ± 1		C
NADH	L-lysine ($2K_m$) α-Kg ($2K_m$)	glutarate	1.1 ± 0.2[b]	1.9 ± 0.4	S-parabolic NC
L-lysine	NADH ($3K_m$) α-Kg ($2K_m$)	glutarate	2.3 ± 0.4		C
α-Kg	NADH ($3K_m$) L-lysine ($2K_m$)	glutarate	1.0 ± 0.1	2.3 ± 0.5	NC

[a] The values in parentheses are the corrected values for the fixed substrates where applicable. [b] Average K_i for binding two molecules of glutarate to E.

NADH is competitive versus NAD and noncompetitive versus saccharopine, while lysine is noncompetitive versus NAD and competitive versus saccharopine. Product inhibition by α-Kg is only observed at high NAD concentrations ($\geq 20K_m$), and it is noncompetitive versus saccharopine. All product inhibition data are summarized in Table 2.

Dead-End Inhibition Studies. Inhibition by leucine, chosen as a dead-end analogue of lysine, was competitive versus lysine, uncompetitive versus NADH, and noncompetitive versus α-Kg. OG was chosen as a dead-end analogue of α-Kg, and it exhibited a competitive inhibition versus α-Kg, uncompetitive inhibition versus NADH, and noncompetitive versus lysine. Oxaloacetate was also chosen as a dead-end analogue of α-Kg, but it is competitive versus lysine, and noncompetitive versus NADH and α-Kg.

When glutarate is used as a dead-end inhibitor, it is competitive versus lysine and noncompetitive versus NADH and α-Kg. The secondary slope replot for glutarate inhibition versus NADH, however, is parabolic, while the intercept replot is linear, indicating S-parabolic noncompetitive inhibition (parts A−C of Figure 4).

Pyruvate is an alternative keto acid substrate but only when both lysine and pyruvate concentrations are very high. Under conditions where inhibition studies are carried out, pyruvate is treated as a dead-end α-Kg substrate analogue. Surprisingly, it shows competitive inhibition versus both lysine and

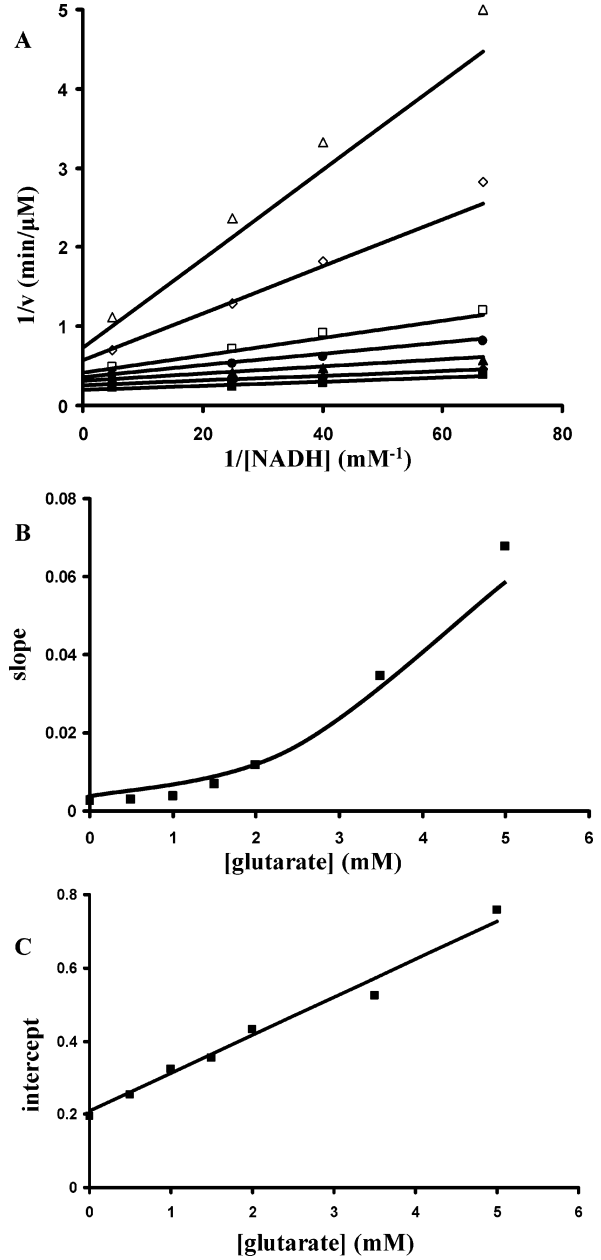

FIGURE 4: S-parabolic noncompetitive inhibition by glutarate against NADH. (A) Primary plot exhibiting the S-parabolic noncompetitive inhibition by glutarate [0 mM (■), 0.5 mM (◆), 1 mM (▲), 1.5 mM (●), 2 mM (□), 3.5 mM (◇), and 5 mM (△)] versus NADH, with lysine and α-Kg fixed at their respective K_m. (B) Secondary plot of the slope versus the glutarate concentration. (C) Secondary plot of the intercept versus the glutarate concentration. Rates were measured in 100 mM Hepes at pH 7.0 and 25 °C. The points are experimental or from a graphical analysis, whereas the solid lines are theoretical based on the kinetic parameters from a fit to eq 10.

α-Kg and uncompetitive inhibition versus NADH. All dead-end inhibition data are summarized in Table 3.

Determination of K_{eq}. With all reactants, with the exception of NAD, fixed as discussed in Materials and Methods, the change in A_{340} (once the system has attained equilibrium after the enzyme was added to the reaction mixture) was plotted against the NAD concentration. The ΔA_{340} is an indicator of the displacement from the equilibrium position (Figure 5). The concentration of NAD that gave a ΔA_{340} of 0 is about

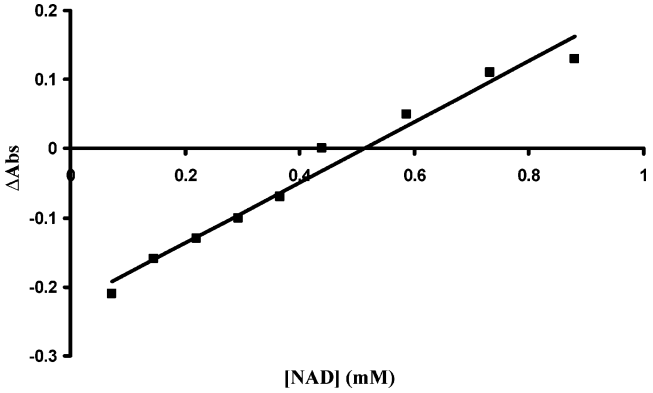

FIGURE 5: Determination of K_{eq}. The difference in A_{340} versus the NAD concentration (0.1−1.2 mM). The points are experimental, while the solid line is theoretical based on a fit to the equation for a straight line.

0.5 mM. The K_{eq} calculated using fixed concentrations of the other reactants and 0.5 mM NAD (eq 11) is 3.9×10^{-7} M, while the K_{eq} calculated from the Haldane relationship is about 2.9×10^{-7} M (eq 12).

DISCUSSION

Initial Velocity Studies. In general, for a sequential terreactant mechanism, the initial velocity patterns obtained by varying concentrations of any two substrates with the third fixed at a nonsaturating concentration are all intersecting. If the second substrate to add in an ordered mechanism is fixed at a saturating concentration, the initial velocity pattern obtained by varying the first substrate at different fixed levels of the last becomes parallel (*19*), while three intersecting patterns would be consistent with a fully random mechanism whatever the concentration of the fixed reactant. Random binding of A and B to E followed by binding of C to EAB also gives intersecting patterns when any of the substrates is saturating and the other two are varied. However, ordered binding of A followed by the random addition of B and C will give two parallel patterns when A and C or A and B are varied at saturating levels of B and C, respectively (*19*).

In the direction of reductive amination of α-Kg catalyzed by SDH, saturation with NADH and varying α-Kg/lysine gave an intersecting pattern, while two parallel patterns were observed for the NADH/α-Kg and NADH/lysine pairs at saturating concentrations of lysine and α-Kg, respectively (parts A−C of Figure 1). These initial velocity patterns suggest the ordered addition of NADH, followed by the random addition of lysine and α-Kg. The binding of NADH to free enzyme has also been demonstrated by isothermal titration calorimetry (ITC) (data not shown). No direct binding of lysine or α-Kg to the free enzyme was detected by ITC, which would result from a high K_d or the lack of a defined binding site in the absence of NADH.

When data from a systematic analysis of initial velocities varying all reactant concentrations were fitted to eq 2 for a fully random terreactant mechanism, the B and C terms in the denominator of the rate equation were not defined, which suggests that the EB (E:α-Kg) and EC (E:lysine) binary complexes are not present. Data are consistent with the above mechanism that suggests that lysine and α-Kg cannot add until NADH does.

The intersecting initial velocity pattern obtained in the direction of saccharopine oxidation indicates a sequential mechanism for the addition of NAD and saccharopine, consistent with data obtained in the opposite direction. The initial velocity data in the absence of added inhibitors do not define the order of addition. Data obtained from initial velocity studies in the direction of saccharopine formation alone do not discriminate between the ordered and random addition of reactants, and thus, the kinetic mechanism was further defined via product and dead-end inhibition studies.

Substrate Inhibition. A number of pyridine nucleotide-linked dehydrogenases are inhibited by high concentrations of the substrates. Generally, the substrate inhibition is considered to be caused by forming a dead-end enzyme:oxidized coenzyme:oxidized substrate complex or a dead-end enzyme:reduced coenzyme:reduced substrate complex. Substrate inhibition resulting from the combination of a substrate with central complexes has also been reported (*20*).

It has been reported that in the reductive amination reaction direction, SDH is inhibited by high concentrations of lysine and α-Kg (both show uncompetitive inhibition against NADH) but not by NADH, while NAD and saccharopine show no substrate inhibition in the physiologic reaction direction (*21*). If the lysine substrate inhibition arises from the formation of a dead-end E:NAD:substrate complex, one would expect uncompetitive inhibition by lysine versus NADH. The observed competitive inhibition by lysine versus NADH indicates that lysine binds to free enzyme at high concentrations, forming a dead-end E:lysine complex.

The substrate inhibition by α-Kg is uncompetitive with respect to NADH at saturating lysine, suggesting a combination to the E:NAD product complex. For α-Kg to cause any substrate inhibition, the E:NAD complex must exist in the steady state, which suggests that the release of NAD from E:NAD contributes to the overall rate limitation at saturating substrate concentrations (V/E_t). Uncompetitive substrate inhibition is common in the nonphysiological direction of a steady-state ordered mechanism (*22*). Whether the inhibition by α-Kg results from the formation of a E:NAD:α-Kg dead-end complex was further tested via a double-inhibition experiment measuring the initial rate at fixed low NADH and lysine and varying the NAD concentration at different inhibitory levels of α-Kg (Figure 3B). The inhibition by NAD alone in Figure 3B is observed as the line with ■ reflecting the E:NAD complex, while the inhibition by α-Kg alone (ordinate) reflects the binding of α-Kg to the E:NAD that exists in the steady state in the absence of added NAD. The slope effect indicates an enhancement of inhibition as a result of synergism of binding between NAD and α-Kg. A value of 0.12 is obtained for α, suggesting an 8-fold increase in the affinity of α-Kg in the presence of NAD, compared to its absence. Under the conditions examined, saccharopine substrate inhibition was not observed over a concentration range of 5−50 mM, in 100 mM Hepes and pH 7.0.

Product Inhibition. The order of product release in the direction of saccharopine formation was examined using product inhibition by NAD and saccharopine. If the overall reaction is reversible and NAD is the last product to leave, the inhibition by NAD would be competitive with respect to NADH and noncompetitive versus the other two substrates. Indeed, inhibition patterns predicted by these assumptions were obtained (Table 2). The competitive inhibition by NAD versus NADH at low lysine and α-Kg indicates that NAD is the last product to leave in the direction of reduction amination. The noncompetitive inhibition by NAD versus the other two reactants is consistent with NAD binding to free enzyme. Thus, the order of product release would be saccharopine followed by NAD. The high K_{ii} value obtained for the noncompetitive inhibition by NAD against α-Kg is likely due to the low concentration of free enzyme (12%), as a result of the high NADH ($3K_m$) and lysine ($2.5K_m$) concentrations used. Correction for the enzyme concentration gives a value of 13 mM, in reasonable agreement with the K_{is} value of 28 mM (Table 2).

According to the proposed mechanism, if saccharopine is the first product to dissociate, one would predict noncompetitive inhibition by saccharopine against all three substrates. However, uncompetitive inhibition by saccharopine versus NADH was observed. The lack of a slope effect can be explained by the combination of saccharopine with E:NADH in dead-end fashion, or with E:NAD with no reversal of the reaction, or both. The noncompetitive patterns observed for saccharopine versus lysine or α-Kg can be explained on the basis of the combination with E:NAD and E:NADH. The inability of saccharopine to reverse the reaction is fully consistent with the K_{eq} of 2.9×10^{-7} M measured for the reaction at pH 7.0. The uncompetitive substrate inhibition by α-Kg and double inhibition by NAD/α-Kg suggest the presence of E:NAD in the steady state, and this is the normal complex with which saccharopine combines as a reactant. It is not unreasonable that saccharopine would bind to the E:NAD and E:NADH complexes because of the structural similarity of the dinucleotide substrates. Both combinations of saccharopine would give an uncompetitive pattern versus NADH and noncompetitive patterns versus lysine and α-Kg. In addition, the high K_{ii} value obtained for the noncompetitive inhibition by saccharopine against α-Kg is likely due to the low concentration of the E:NAD complex to which saccharopine binds, as a result of the low NADH (K_{NADH}) and lysine (K_{Lys}) concentrations used.

In the direction of saccharopine oxidation, all products were used as product inhibitors. The inhibition by α-Kg was only observed when NAD is saturating ($20K_m$) and resulted largely from the formation of the abortive E:NAD:α-Kg complex (see the discussion of double-inhibition experiments above). The combination of α-Kg with E:NAD would be expected to give competitive inhibition versus saccharopine, and the combinations of α-Kg with E:NADH and E:NADH:lysine enzyme forms would give noncompetitive inhibition. The observed noncompetitive inhibition pattern is thus consistent with the proposed mechanism. The high K_{ii} value results from the low concentrations of E:NADH and E:NADH:lysine complexes present in the steady state (saccharopine fixed at $1.5K_{sacc}$).

The product NADH exhibits competitive inhibition against NAD, suggesting that NADH and NAD bind to free enzyme. NADH exhibits noncompetitive inhibition versus saccharopine, consistent with NADH binding before saccharopine along the reaction pathway, in accordance with the proposed mechanism, that is, the addition of NAD before saccharopine.

Lysine is competitive versus saccharopine under conditions where NAD is fixed at its K_m. It thus appears that no significant E:NADH or E:NADH:α-Kg is present in the steady state under these conditions. This is consistent with

Scheme 1: Schematic of the Saccharopine-Binding Pocket To Illustrate Possible Inhibition Binding Modes[a]

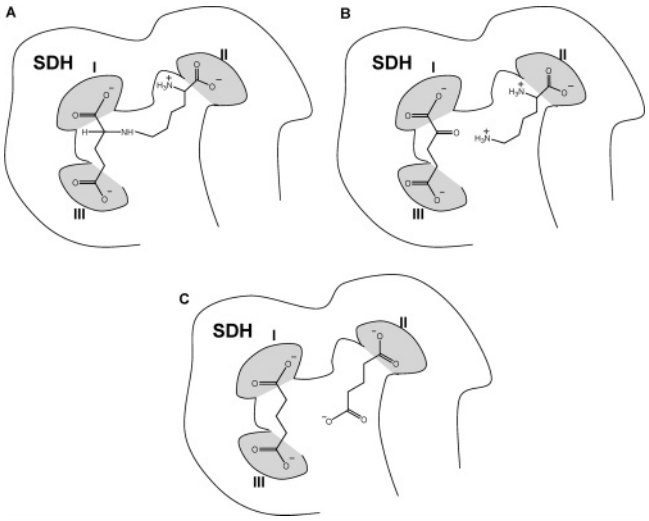

[a] A and B show a possible binding pocket for saccharopine, lysine, and α-Kg. C shows possible binding modes for glutarate.

the lack of substrate inhibition by saccharopine (see above). The noncompetitive inhibition versus NAD then results from the combination of lysine with E (see lysine substrate inhibition above) and E:NAD when higher lysine concentrations are used.

Dead-End Inhibition. Dead-end inhibitors structurally resemble the substrate and compete with the substrate for a binding site on the enzyme; however, they do not undergo chemical transformation like the substrate. As a result, it is often more straightforward to interpret data from dead-end inhibition, and these experiments are invaluable in establishing the order of substrate binding (*23*).

Leucine was chosen as a dead-end analogue of lysine and was competitive versus lysine, indicating that it competes with lysine for its binding site on the enzyme. The uncompetitive inhibition observed versus NADH is consistent with leucine binding to a form of enzyme that exists when NADH is saturating. The noncompetitive inhibition against α-Kg results from the combination with an enzyme form that α-Kg binds and one that is present at saturating α-Kg, viz., the E:NADH and E:NADH:α-Kg enzyme forms. All of the leucine dead-end patterns are consistent with the random addition of lysine and α-Kg once NADH is bound.

OG was chosen as a dead-end analogue of α-Kg. It was competitive versus α-Kg, indicating that it competes with α-Kg for its binding site on the enzyme. The uncompetitive inhibition observed versus NADH is consistent with OG binding to a form of the enzyme that exists when NADH is saturating. The noncompetitive inhibition against lysine results from the combination of E:NADH and E:NADH:lysine enzyme forms. All of the OG dead-end patterns are consistent with the random addition of lysine and α-Kg once NADH is bound.

OAA was also chosen as a dead-end analogue of α-Kg. However, OAA exhibited behavior similar to that of leucine. It was competitive versus lysine, suggesting that it binds to the same enzyme form(s) as does lysine. However, it was noncompetitive versus both α-Kg and NADH, suggesting that it binds to E as well as the E:NADH and E:NADH:α-Kg enzyme forms.

Glutarate as a dead-end inhibitor is competitive versus lysine and noncompetitive versus α-Kg, as are leucine and OAA. However, it exhibits S-parabolic noncompetitive inhibition versus NADH. Thus, in addition to binding to E:NADH and E:NADH:α-Kg, glutarate binds to E, as does OAA. The parabolic slope effect indicates the formation of a E:$(\text{glutarate})_2$ complex, likely as a result of occupying both the lysine- and α-Kg-binding sites. This is a reasonable result because glutarate can be seen as a mimic of both halves of saccharopine. Attempts to fit the data using eq 13 were unsuccessful, giving a K_{i1} higher than the concentration range used for glutarate and a K_{i2} lower than the concentration range used.

$$v = \frac{\mathrm{V}\mathbf{A}}{K_a\left(1 + \frac{\mathbf{I}}{K_{i1}} + \frac{\mathbf{I}^2}{K_{i1}K_{i2}}\right) + \mathbf{A}\left(1 + \frac{\mathbf{I}}{K_{ii}}\right)} \qquad (13)$$

In eq 13, K_{i1} and K_{i2} are dissociation constants for glutarate from the E:glutarate and E:$(\text{glutarate})_2$ complexes, respectively. A fit to eq 10, a modified version of eq 13, with the $\mathbf{I}/K_{i1}$ term missing, gives good estimates and indicates that the first molecule of glutarate bound has a very low affinity, while the second glutarate molecule bound increases the affinity of the first dramatically, trapping it on the enzyme. As a result, an average K_{is} is obtained for dissociation of both molecules from the E:$(\text{glutarate})_2$ complex.

Pyruvate was reported as a slow alternative keto acid substrate (*15*, *16*). Enzyme activity with pyruvate was observed in these studies only when the lysine concentration was fixed at 40 times the value of K_{Lys} obtained for the

Scheme 2: Proposed Kinetic Mechanism for the SDH[a]

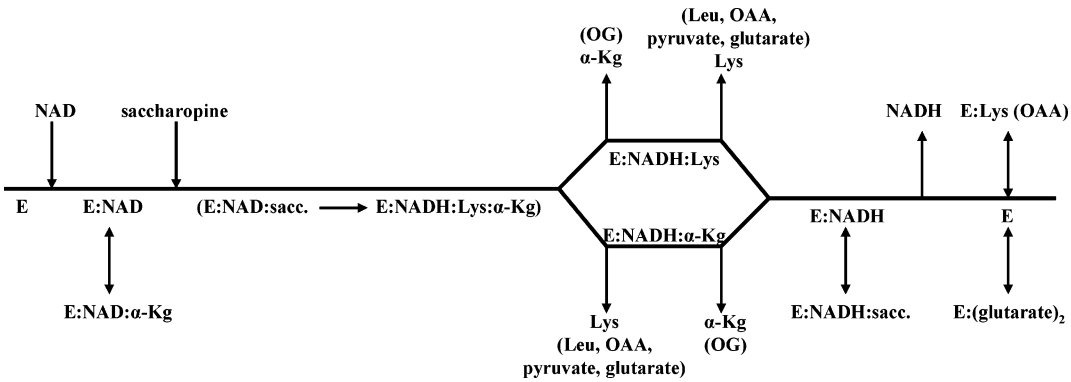

[a] E represents the SDH. Kinetic data suggest that the reaction is irreversible in agreement with the K_{eq} of the reaction. Inhibitor(s) within parenthesis all bind to the same enzyme form as does Lys.

normal reaction using α-Kg, and a pyruvate concentration is 200 times higher than α-Kg needed for the normal reaction. As a result, pyruvate is treated as a dead-end analogue of α-Kg. Surprisingly, it shows competitive inhibition versus both lysine and α-Kg and uncompetitive inhibition versus NADH, indicating that it binds to both E:NADH:α-Kg and E:NADH:lysine enzyme forms, so that it, like glutarate, binds to both subsites occupied by saccharopine.

The binding mode of the two glutarate molecules in the E:(glutarate)$_2$ complex and the competitive inhibition patterns observed for pyruvate versus both lysine and α-Kg are reasonable considering that their structure mimics both reactants, in part, i.e., α-keto acid and dicarboxylic acid. A schematic representation of the saccharopine-binding pocket is shown in Scheme 1. There are likely three subsites (I, II, and III) for the interaction of the three carboxylates of saccharopine (Scheme 1A). Production of lysine and α-Kg would then give their binding modes as in Scheme 1B. Binding of glutarate may then be accommodated at both sites as shown in Scheme 1C. It is also possible that binding sites I and II could be used by one molecule of glutarate and III for a second.

On the basis of the initial velocity studies in the absence and presence of product and dead-end inhibitors, SDH has a relatively flexible and large substrate-binding pocket for saccharopine and its products, lysine and α-Kg. The binding of NADH causes a conformational change, increasing the affinity of the enzyme for lysine and α-Kg as indicated by the difference in the substrate inhibition constant and the K_m (steady-state dissociation constant) for lysine. An overall kinetic mechanism can thus be proposed and is shown in Scheme 2. For the fully defined kinetic mechanism, the rate equation in the direction of saccharopine formation (eq 3) can be defined in terms of kinetic constants as shown in eq 14

$$v = \frac{V\mathbf{ABC}}{K_{ia}K_{ib}K_c + K_{ib}K_c\mathbf{A} + K_b\mathbf{AC} + K_c\mathbf{AB} + K_a\mathbf{BC} + \mathbf{ABC}} \quad (14)$$

In eq 14, K_{ia} and K_{ib} are dissociation constants of A from EA and B from EAB complexes, respectively, and all other terms are the same as defined above. A refit of all initial velocity data in the direction of saccharopine formation using eq 14 gives K_{ia} a value of 0.018 ± 0.004 mM and K_{ib} a value of 0.6 ± 0.1 mM. All other constants are given in Table 1.

Quantitative Analysis of Dead-End Inhibition Data. For dead-end inhibitors, the correction of the observed K_i values for the fixed substrate concentrations should give the same K_i value whatever substrate is varied. Thus, for inhibition by OG and leucine, the observed K_{is} and K_{ii} values must be corrected for the concentration of the fixed substrates. We give an example of how this is done below. Given eq 14, each of the terms in the denominator represents an enzyme form. The EA and EAC forms of the enzyme bound OG, represented by $K_{ib}K_c\mathbf{A}$ and $K_b\mathbf{AC}$, respectively, and these terms would be multiplied by $(1 + \mathbf{I}/K_{i1})$ and $(1 + \mathbf{I}/K_{i2})$, respectively, where **I** is OG and K_{i1} and K_{i2} are dissociation constants for E:NADH:OG and E:NADH:Lys:OG, respectively. However, because $K_{i1} = K_{i2}$ in this case (see below), eq 15 is correct. The presence of the inhibitor adds a $(1 + \mathbf{I}/K_i)$ term to each of the denominator terms representing EA and EAC enzyme forms to which B binds, $K_{ib}K_c\mathbf{A}$ and $K_b\mathbf{AC}$, to give eq 15, where K_i is the intrinsic dissociation constant for inhibitors

$$v = \frac{V\mathbf{ABC}}{K_{ia}K_{ib}K_c + (K_{ib}K_c\mathbf{A} + K_b\mathbf{AC})\left(1 + \frac{\mathbf{I}}{K_i}\right) + K_c\mathbf{AB} + K_a\mathbf{BC} + \mathbf{ABC}} \quad (15)$$

With **B** varied, eq 15 in double-reciprocal form is given by eq 16

$$\frac{1}{v} = \left[\frac{K_{ia}K_{ib}K_c}{V\mathbf{AC}} + \left(\frac{K_{ib}K_c}{V\mathbf{C}} + \frac{K_b}{V}\right)\left(1 + \frac{\mathbf{I}}{K_i}\right)\right]\left(\frac{1}{\mathbf{B}}\right) + \left[\frac{K_a}{\mathbf{A}} + \frac{K_c}{\mathbf{C}} + \frac{1}{V}\right] \quad (16)$$

The expression for the slope of eq 16 versus **I** is given in eq 17

$$\text{slope} = \left(\frac{K_{ia}K_{ib}K_c}{V\mathbf{AC}} + \frac{K_{ib}K_c}{V\mathbf{C}} + \frac{K_b}{V}\right) + \left(\frac{K_{ib}K_c}{VK_i\mathbf{C}} + \frac{K_b}{VK_i}\right)\mathbf{I} \quad (17)$$

and with slope equal to 0

$$\mathbf{I} = \text{app}K_{is} = -K_i\left(\frac{\frac{K_{ia}K_{ib}K_c}{V\mathbf{AC}} + \frac{K_{ib}K_c}{V\mathbf{C}} + \frac{K_b}{V}}{\frac{K_{ib}K_c}{V\mathbf{C}} + \frac{K_b}{V}}\right) \quad (18)$$

where the appK_{is} values are those given in Table 3.

With **A** varied, eq 15 in double-reciprocal form is given by eq 19

$$\frac{1}{v} = \left(\frac{K_{ia}K_{ib}K_c}{V\mathbf{BC}} + \frac{K_a}{V}\right)\left(\frac{1}{\mathbf{A}}\right) + \left[\left(\frac{K_{ib}K_c}{V\mathbf{BC}} + \frac{K_b}{V\mathbf{B}}\right)\left(1 + \frac{\mathbf{I}}{K_i}\right) + \frac{K_c}{V\mathbf{C}} + \frac{1}{V}\right] \quad (19)$$

The expression for the intercept of eq 19 versus **I** is given in eq 20

$$\text{intercept} = \left(\frac{K_{ib}K_c}{V\mathbf{BC}} + \frac{K_b}{V\mathbf{B}} + \frac{K_c}{V\mathbf{C}} + \frac{1}{V}\right) + \left(\frac{K_{ib}K_c}{VK_i\mathbf{BC}} + \frac{K_b}{VK_i\mathbf{B}}\right)\mathbf{I} \quad (20)$$

and with intercept equal to 0

$$\mathbf{I} = \text{app}K_{ii} = -K_i\left(\frac{\frac{K_{ib}K_c}{V\mathbf{BC}} + \frac{K_b}{V\mathbf{B}} + \frac{K_c}{V\mathbf{C}} + \frac{1}{V}}{\frac{K_{ib}K_c}{V\mathbf{BC}} + \frac{K_b}{V\mathbf{B}}}\right) \quad (21)$$

With **C** varied, the expression for K_{is} and K_{ii} can be derived in a similar manner and the true K_i can be calculated. Values of K_{i1} and K_{i2} are obtained by correcting the slope (K_{is}) and intercept (K_{ii}) values measured for the noncompetitive inhibition versus lysine (Table 3). Note that these values,

0.07 and 0.06 mM are identical within error, justifying the use of eq 15 above. The corrected values of K_i are given in parentheses in Table 3, and all are in very good agreement with one another.

Similar corrections have been done for leucine inhibition patterns and could be carried out for all other dead-end inhibition patterns, but this serves to illustrate the process. Data are then consistent with the proposed kinetic mechanism.

Previously Published Data. Previously, an ordered kinetic mechanism was proposed for SDH (*13*, *14*). Data suggested that when α-Kg was used as the keto acid substrate, the mechanism was defined as ordered with NAD bound first, followed by saccharopine, and products were released in the order lysine, α-Kg, and NADH. However, when α-Kg was substituted by the alternative slow keto acid substrate pyruvate, the mechanism was still ordered but with the order of product release pyruvate, lysine, and NADH (*16*). In addition, one of the pairwise initial velocity patterns obtained by the authors, NADH/lysine at saturating levels of α-Kg, was not consistent with the proposed ordered mechanism (*12*). Noncompetitive inhibition patterns observed with OAA, pyruvate, α-ketobutyrate, α-ketovalerate, and α-ketocaproate were observed previously (*14*), whether NADH, α-Kg, or lysine was the varied substrate, and these patterns are also inconsistent with a sequential ordered kinetic mechanism. The ordered mechanism proposed previously differs from that proposed on the basis of studies presented here. Previous results fit well into the mechanism that we propose. The keto acid substrates bind to E:NADH and E:NADH:lysine complexes, consistent with the random addition of the keto acid substrate and lysine. In addition, however, a number of dead-end complexes exist that were not observed previously, and some mono- and dicarboxylic acid inhibitors can apparently bind to both subsites of the saccharopine-binding site (Scheme 1).

Differences between the previous studies and those in this paper may be caused by a number of reasons. The specific activity of the His-tagged SDH in this study is 243.9 units/mg, more than twice the value of 130 units/mg reported in previous studies (*12*). Hepes buffer was used in all of the studies presented, rather than the phosphate buffer used previously, to eliminate possible inhibition by phosphate. A systematic analysis of initial velocities that covers limiting and saturating concentrations of all three reactants at once was performed in this study in addition to the pairwise analysis. Finally, the kinetic mechanism was probed in both reaction directions as opposed to the reductive amination direction alone.

Interestingly, inhibition patterns obtained differ between the two studies, and this appears to be largely a result of the conditions utilized. For example, a lack of inhibition by glutarate as a dead-end analogue was reported previously (*14*), and this is almost certainly due to the limited glutarate concentration range examined and the unique type of inhibition in which two molecules of glutarate are apparently needed for significant affinity. All of the inhibition patterns obtained in these studies can be reconciled on the basis of the promiscuity of the saccharopine-binding site. Overall, the present studies present a complete description of the kinetic mechanism of SDH at pH 7.0.

REFERENCES

1. Xu, H., Andi, B, Qian, J, West, A. H., and Cook, P. F. (2006) The α-aminoadipate pathway for lysine biosynthesis in fungi, *Cell Biochem. Biophys. 46*, 43−64.
2. Zabriskie, T. M., and Jackson, M. D. (2000) Lysine biosynthesis and metabolism in fungi, *Nat. Prod. Rep. 17*, 85−97.
3. Nishida, H., Nishiyama, M., Kobashi, N., Kosuge, T., Hoshino, T., and Yamane, H. (1999) A prokaryotic gene cluster involved in synthesis of lysine through the aminoadipate pathway: A key to the evolution of amino acid biosynthesis, *Genome Res. 9*, 1175−1183.
4. Bhattacharjee, J. K. (1985) α-Aminoadipate pathway for the biosynthesis of lysine in lower eukaryotes, *Crit. Rev. Microbiol. 12*, 131−151.
5. Bhattacharjee, J. K. (1992) Evolution of the α-aminoadipate pathway for the synthesis of lysine in fungi, in *Evolution of Metabolic Function* (Mortlock, R. P., Ed.), pp 47−80, CRC Press, Boca Raton, FL.
6. Strassman, M., and Weinhouse, S. (1953) Biosynthetic pathways. III. The biosynthesis of lysine in *Torulopsis utilis*, *J. Am. Chem. Soc. 75*, 1680−1684.
7. Vogel, H. J. (1965) Lysine biosynthesis and evolution, in *Evolving Genes and Proteins* (Bryson, V., Ed.), pp 25−40, Academic Press, New York.
8. Garrad, R. C., and Bhattacharjee, J. K. (1992) Lysine biosynthesis in selected pathogenic fungi: Characterization of lysine auxotrophs and the cloned *LYS1* gene of *Candida albicans*, *J. Bacteriol. 174*, 7379−7384.
9. Johansson, E., Steffens, J. J., Lindqvist, Y., and Schneider, G. (2000) Crystal structure of saccharopine reductase from *Magnaporthe grisea*, an enzyme of the α-aminoadipate pathway of lysine biosynthesis, *Structure 8*, 1037−1047.
10. Ye, Z. H., and Bhattacharjee, J. K. (1988) Lysine biosynthesis pathway and biochemical blocks of lysine auxotrophs of *Schizosaccharomyces pombe*, *J. Bacteriol. 170*, 5968−5970.
11. Ogawa, H., and Fujioka, M. (1978) Purification and characterization of saccharopine dehydrogenase from baker's yeast, *J. Biol. Chem. 253*, 3666−3670.
12. Fujioka, M., and Nakatani, Y. (1974) Saccharopine dehydrogenase, a kinetic study of coenzyme binding, *J. Biol. Chem. 249*, 6886−6891.
13. Fujioka, M., and Nakatani, Y. (1970) A kinetic study of the saccharopine dehydrogenase reaction, *Eur. J. Biochem. 16*, 180−186.
14. Fujioka, M., and Nakatani, Y. (1972) Saccharopine dehydrogenase, interaction with substrate analogues, *Eur. J. Biochem. 25*, 301−307.
15. Fujioka, M., and Tanaka, M. (1978) Enzymic and chemical synthesis of ϵ-N-(L-propionyl-2)-L-lysine, *Eur. J. Biochem. 90*, 297−300.
16. Sugimoto, K., and Fujioka, M. (1978) The reaction of pyruvate with saccharopine dehydrogenase, *Eur. J. Biochem. 90*, 301−307.
17. Bishop, C. M. (1995) *Neural Networks for Pattern Recognition*, Oxford University Press: Oxford, U.K.
18. Viola, R. E., and Cleland, W. W. (1982) Initial velocity analysis for terreactant mechanisms, *Methods Enzymol. 87*, 353−366.
19. Cleland, W. W. (1970) Steady-state enzyme kinetics, in *The Enzymes* (Boyer, P. D., Ed.) Vol. 2, pp 1−65, Academic Press, New York.
20. Northrop, D. B., and Cleland, W. W. (1974) The kinetics of pig heart triphosphopyridine nucleotide-isocitrate dehydrogenase. II. Dead-end and multiple inhibition studies, *J. Biol. Chem. 249*, 2928−2931.
21. Fujioka, M. (1975) Saccharopine dehydrogenase, substrate inhibition studies, *J. Biol. Chem. 250*, 8986−8989.
22. Yonetani, T., and Theorell, H. (1964) Studies on liver alcohol dehydrogenase complexes. III. Multiple inhibition kinetics in the presence of two competitive inhibitors, *Arch. Biochem. Biophys. 106*, 243−251.
23. Cleland, W. W. (1977) Determining the chemical mechanisms of enzyme-catalyzed reactions by kinetic studies, *Adv. Enzymol. Relat. Areas Mol. Biol. 45*, 273−387.

BI0610808